Peculiarities of laser melting and evaporation of superconducting ceramics

V. Mazhukin
Institute of Mathematical Modelling, Russian Academy of Sciences, Miusskaya Square, 4, 125047 Moscow (Russian Federation)
I. Smurov
Ecole Nationale d'Ingénieurs de Saint-Etienne, 58 rue Jean Parot, 42023 Saint-Etienne (France)
G. Flamant and C. Dupuy
Institut de Science et de Génie des Matériaux et Procédés, C.N.R.S., B.P. No. 5, 66125 Font-Romeu Cédex (France)

Abstract

Pulsed laser melting and evaporation of superconducting ceramics is simulated numerically. The dynamics of both phase fronts (evaporation and melting/solidification) are analysed during the whole thermal cycle. The appearance of overheated metastable states in the solid and liquid phases as a result of the phase front dynamics and the volume nature of laser energy release is shown. The influence of the volume absorption coefficient (or wavelength of laser radiation) on heat phenomena is analysed.

1. Introduction

Pulsed laser deposition (PLD) of thin superconducting films for electronic device applications (such as compact high quality factor filters, delay lines, Josephson elements for high-speed, low-power switching) is a modern and successfully developed technology [1–3].

The related physical phenomena include volume absorption of laser radiation, heating, melting and evaporation of the target material, plasma formation, laser beam–plume interaction etc., and, finally, the deposition of thin films on a substrate in a vacuum chamber (100–300 mTorr of oxygen). Although PLD operations are well-developed there remain difficulties. The micron-sized particles generated by splashing are a major problem detrimental to film quality. Moreover, difficulties are increased because of (a) poor predictability of the final experimental results, due mainly to an incomplete knowledge of the physics and chemistry of related processes; and (b) the lack of knowledge concerning the thermophysical properties and high-temperature chemistry of superconducting ceramics. Experimental methods are not yet capable of revealing the dynamics of PLD because of its short duration and small size of action. The role of mathematical modelling in such a situation is to develop a numerical experiment instead of a real one. In the present article a possible reason for particle generation by splashing in PLD is proposed and analysed by means of numerical experiments.

2. Mathematical model

Laser radiation is spread along the x-axis. The solid–liquid and liquid–vapour interfaces are located at points $x = \Gamma_{sl}$ and $x = \Gamma_{lv}$, respectively. The laser beam is partially absorbed by the irradiated material, which can be heated, melted or evaporated depending on the radiation intensity and pulse duration. Generally, the distinction between volumetric and surface energy absorption of electromagnetic radiation comes from the relative importance of radiative energy transport and conductive heat transfer. These phenomena can be characterized by the mean path length of photons in the medium, l_p ($l_p \sim 1/\chi$, where χ is the absorption coefficient), and the thermal penetration depth $l_T \sim (at)^{1/2}$. If $l_T \gg l_p$, the radiation transformation into thermal energy is located at the surface. On the contrary, if $l_T \leqslant l_p$ the energy absorption occurs in a volume. The volumetric heating may also appear during phase transformation, if $\chi a / v_{sl} \leqslant 1$.

The volume absorption of laser radiation is described by the combined system of energy and radiation transfer equations:

$$C_p(T)\rho(T)\frac{\partial T}{\partial t} = \frac{\partial}{\partial x}\lambda(T)\frac{\partial T}{\partial x} - \frac{\partial G}{\partial x} \tag{1}$$

$$\frac{\partial G}{\partial x} + \chi G = 0 \tag{2}$$

0040-6090/94/$7.00
SSDI 0040-6090(93)03724-Y

On the irradiated surface $x = x_L$ the following boundary conditions occur:

$$\lambda \frac{\partial T}{\partial x} = 0 \tag{3a}$$

$$G_s = A(T_s)G_0 \tag{3b}$$

With surface energy absorption the heat transfer eqn. (1) does not contain the term $\partial G/\partial x$, and the equation for radiation transfer is not required. In this case laser action is taken into account in the boundary conditions (3a) and (3b) expressing the law of energy conservation. Taking into consideration the above statements, the mathematical model describing the behaviour of solid (s) and liquid (l) phases accounting for phase transformations can be written as follows [4]:

$$\left(C_p(T)\rho(T)\frac{\partial T}{\partial t}\right)_k = \left(\frac{\partial}{\partial x}\lambda(T)\frac{\partial T}{\partial x} - \frac{\partial G}{\partial x}\right)_k, \quad k = s,l \tag{4a}$$

$$\left(\frac{\partial G}{\partial x} + \chi G\right)_k = 0, \quad -t_0 < t < t_j, \quad x_0 < x < x_L \tag{4b}$$

The boundary conditions are, at $t = -t_0$:

$$T(x, 0) = T_0 \tag{5a}$$

at $x = x_0$:

$$\lambda \frac{\partial T}{\partial x} = 0 \tag{5b}$$

at $x = \Gamma_{sl}$:

$$\lambda_s \frac{\partial T_s}{\partial x} - \lambda_l \frac{\partial T_l}{\partial x} = \rho_l L_m v_{sl}, \quad T_s = T_l = T_m \tag{5c}$$

and at $x = \Gamma_{lv}$:

$$-\lambda_l \frac{\partial T_l}{\partial x} = \rho_l L_v v_{lv}, \quad G_s = A(T_s)G_0 \exp[-(t/\tau)^2] \tag{5d}$$

$$\rho_l v_{lv} = \rho_v(v_{lv} - u) \tag{6}$$

$$P_l + \rho_l v_v^2 = P_v + \rho_v(v_{lv} - u)^2 \tag{7}$$

$$T_v = T_l\left\{\left[1 + \pi\left(\frac{\gamma - 1}{\gamma + 1}\frac{m}{2}\right)^2\right]^{1/2} - \pi^{1/2}\frac{\gamma - 1}{\gamma + 1}\frac{m}{2}\right\}^2 \tag{8}$$

$$\rho_v = \rho_H\left\{\left(\frac{T_l}{T_v}\right)^{1/2}\left[(m^2 + 1/2)\exp(m^2)\mathrm{erfc}(m) - \frac{m}{\pi^{1/2}}\right] + \frac{1}{2}\frac{T_l}{T_v}[1 - \pi^{1/2} m \exp(m^2)\mathrm{erfc}(m)]\right\} \tag{9}$$

$$m = \frac{u}{(2RT_v)^{1/2}} \tag{10}$$

$$M = m\left(\frac{2}{\gamma}\right)^{1/2} \tag{11}$$

$$P_H = R\rho_H T_l \tag{12}$$

$$P_H = P_b \exp\left[\frac{L_v}{RT_l}\left(1 - \frac{T_b}{T_l}\right)\right] \tag{13}$$

In these equations a is the thermal diffusivity; $A(T_s)$ is the surface absorptivity; C_p is the heat capacity; G is the energy density flux; G_s is the absorbed energy density flux; G_0 is the maximum value of the incident energy density flux; L_m is the latent heat of melting; L_v is the latent heat of evaporation; M is the Mach number; P is the pressure; R is the universal gas constant; t is the time; $-t_0$ and t_j are the limits of time variation; $T(x, t)$ is the temperature; T_0 is the initial temperature; T_m is the melting point; u is the vapour velocity; v_{sl} is the velocity of the solid–liquid interface; v_{lv} is the velocity of the liquid–vapour interface; x is the spatial coordinate; x_0 and x_L are the limits of coordinate variation; γ is the ratio of heat capacities; Γ_{sl} is the solid–liquid interface; Γ_{lv} is the liquid–vapour interface; χ is the volumetric absorption coefficient of laser radiation; λ is the thermal conductivity; ρ is the density; and τ is the effective pulse duration in the Gaussian distribution used in the approximation of laser pulse shape. The subscripts are: b (boiling point), H (saturated vapour), l (liquid phase), s (condensed phase) and v (gas phase).

The evaporation process is described within the approximation of the Knudsen layer, presented as the gas dynamic discontinuity on the phase boundary at $x = \Gamma_{lv}$, where three conservation laws (energy, mass and momentum, respectively) and two additional relations (characterizing the non-equilibrium degree of the phase boundary) are used [5]. In the present work, evaporation into a vacuum is considered, and as a result $M = 1$.

3. Numerical solution

The numerical algorithm is based on the method of dynamic adaptation of the computational grid for the sought solution (specially developed for Stefan-type problems [6, 7]). In the dynamic adaptation method the problem of the computational grid construction is formulated at a differential level. In the differential problem one part of the equations describes the physical processes and the other one the displacement of the grid points.

It is necessary to emphasize that different methods of computational grid construction, based on the various adaptation mechanisms, are developed (for example, refs. 8–11). Notice that the simulation of Stefan-type problems, with volume energy release and with the explicit tracking of phase fronts positions, as in the present article, is the most precise.

The application of dynamic adaptation permits us to develop a numerical algorithm the main idea of which is to make calculations according to a shock-fitting

scheme with simultaneous front tracking [12]. For this purpose the solution of the corresponding difference scheme at one time step is done by means of two enclosed iteration cycles.

4. Results and discussion

Consider the typical conditions of pulsed laser evaporation of ceramics, such as $YBa_2Cu_3O_{7-x}$. It is known that the corresponding optical and thermophysical properties depend poorly on temperature and their values are within the range $\chi = 10^4 - 10^5\ \mathrm{cm}^{-1}$, $C_p = 3 - 8 \times 10^{-1}\ \mathrm{J\,g^{-1}\,K^{-1}}$ and $\lambda = 1 - 5 \times 10^{-2}\ \mathrm{W\,cm^{-1}\,K^{-1}}$. Thus ceramics are materials with low thermal diffusivity (compared with metals), and relatively high absorption coefficient (compared with dielectrics). The experiments show that $YBa_2Cu_3O_{7-x}$ is evaporated through the melting state, *i.e.* as are most metals. However, due to the different relationship between the parameters a and χ, laser energy absorption in ceramics is of a substantially volumetric type.

In calculations, because of the absence of reliable data on optical and thermophysical characteristics and parameters, all the values are assumed to be constant and the same for both phases: $T_m = 1300$ K, $T_v = 2000$ K, $L_m = 2.5 \times 10^2\ \mathrm{J\,g^{-1}}$, $L_v = 6 \times 10^3\ \mathrm{J\,g^{-1}}$, $\rho_s = \rho_l = 6.43\ \mathrm{g\,cm^{-3}}$, $\lambda_s = \lambda_l = 3 \times 10^{-2}\ \mathrm{W\,cm^{-1}\,K^{-1}}$, $A_s = A_l = 80\%$, $C_{p_s} = C_{p_l} = 5 \times 10^{-1}\ \mathrm{J\,g^{-1}\,K^{-1}}$ and $\chi = 5 \times 10^4\ \mathrm{cm}^{-1}$.

The problem of examination of the thermophysical properties of ceramics (as mentioned above) requires special consideration, which is not presented in this paper.

The simulation was performed for melting and evaporation of the ceramic target (thickness 5 μm) by a laser pulse with the following parameters: $\tau = 50$ ns and $G_0 = 10^7\ \mathrm{W\,cm^{-2}}$. The real temporal shape of the laser pulse is approximated by a Gaussian distribution. Hence it is convenient to measure time with respect to the middle of the pulse, *i.e.* $t = 0$ corresponds to its mid-point. In this case, the time before the middle of the pulse is negative, and the time after is positive. Because of the low conductivity of the ceramic material (and the short pulse duration), its initial thickness is large enough so we can neglect the boundary condition on the back side. Therefore, the heat transfer processes considered correspond in practice to those of a semi-infinite body.

Let us compare both temperature profiles in the case of volumetric and surface absorption of radiation, at the beginning of melting: the former is characterized by a smoother distribution in space and lower spatial gradients, and as a result the melting velocity, v_{sl}, increases more slowly with time. The melting process

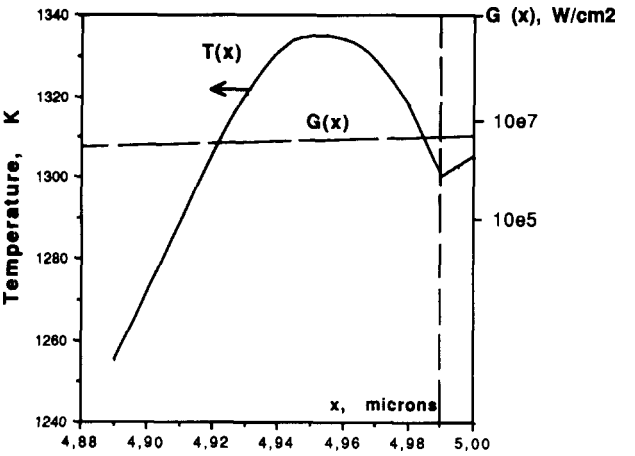

Fig. 1. Spatial temperature distribution (T) at $t = -32.4$ ns (with respect to the middle of the pulse), $\chi = 5 \times 10^4\ \mathrm{cm}^{-1}$ and $\tau = 50$ ns. The vertical dashed line is the position of melting front and the spatial distribution of the absorbed energy density flux G is shown by the dashed curve. The right boundary corresponds to the position of irradiated surface.

starts from the irradiated surface and rapidly leads to the temperature maximum appearing in the depth of the solid phase because of the volumetric heat source (Fig. 1). Its temperature is 50° above the melting point T_m. As a result, a solid phase region (size about 0.1 μm) is formed where the substance is in an overheated metastable state. The size of the overheated region and the degree of overheating generally depend on the thermal diffusivity, absorptivity and heat source intensity. For example, the sub-surface temperature maximum can reach 1466 K (166 K overheating of solid phase above the melting point) at a 0.237 μm depth ($\chi = 10^4\ \mathrm{cm}^{-1}$, $\tau = 40$ ns, $t = 29.7$ ns, and all the other parameters are the same as before). It is necessary to emphasize that detection of the above-mentioned effect is not possible without explicit tracking of the melting front position. Notice that the overheating of the solid state is absent in the case of surface absorption of laser radiation (for example, in action on metallic materials, even with explicit tracking of the phase front positions [13–15]).

During heating, the thickness of the liquid phase rapidly increases and reaches 0.3 μm at $t = 13.5$ ns, which corresponds to a maximum value of the evaporation velocity of $0.94\ \mathrm{m\,s^{-1}}$ ($\chi = 10^5\ \mathrm{cm}^{-1}$, $\tau = 40$ ns, and all the other parameters are the same as before). The increase of the liquid phase thickness leads to a greater absorption of radiation inside the melt, resulting in its further heating, up to a temperature comparable to the boiling point. At the same time, a relatively small proportion of the radiation reaches the solid phase and the degree of its overheating (because of heat transfer) decreases until it disappears completely. Liquid phase surface evaporation on the one hand, and volume en-

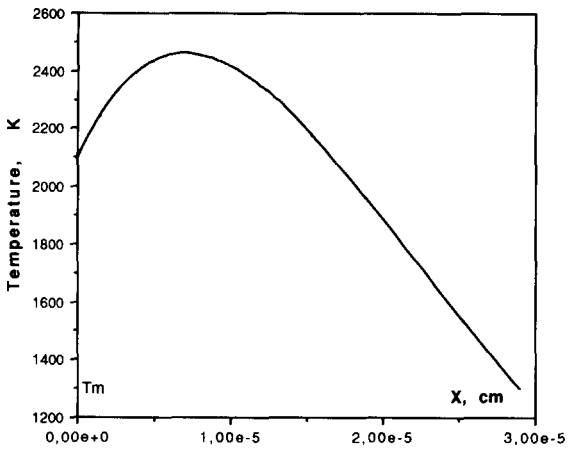

Fig. 2. Spatial temperature distribution in the liquid phase at $t = -13.5$ ns (with respect to the middle of the pulse), $\chi = 10^5\ \mathrm{cm}^{-1}$ and $\tau = 40$ ns. This moment corresponds to the maximum of evaporation front velocity. The left boundary corresponds to the position of the irradiated surface.

ergy absorption on the other lead to the formation of the new sub-surface temperature maximum (Fig. 2). The value of $\chi = 10^5\ \mathrm{cm}^{-1}$ corresponds to a laser wavelength of about $\lambda = 0.1$ μm.

Let us discuss the (P, T) values as calculated from the model (eqns. (4)–(13)). For a given P, the calculated surface temperature is higher than that at equilibrium (from the P, T phase diagram). This means that the irradiated surface is overheated relative to equilibrium conditions. Hence, the occurrence of the sub-surface temperature maximum in the liquid phase probably indicates the formation of a new metastable region. Contrary to solid phase overheating, the metastable state in the liquid is maintained practically until the end of the pulse. The sub-surface maximum of temperature in the melt is absent (even when intensive evaporation takes place) in the case of surface absorption of laser radiation. This means that $\chi \to \infty$, which for ceramics corresponds to the decrease of laser wavelength, or, on the other hand, to laser action on metallic materials [13–15].

In a general case the evolution of the spatial temperature distribution in both the liquid and solid phases can be divided into three main stages: (a) a sub-surface temperature maximum in the solid phase at the initial stage of melting; (b) the existence of two temperature maxima, one in the liquid and the other in the solid phase; and (c) complete disappearance of the temperature maximum in the solid phase, whereas in the liquid phase it exists practically until the end of the pulse.

It is necessary to note that in the present heat transfer model (eqns. (4)–(13)) processes related to volumetric liquid phase nucleation and volumetric vapour formation are not considered. A detailed study of the kinetics of these phenomena is not yet possible. Moreover, in the heat transfer model it is supposed that the metastable phase is stable enough and has no time to decay during pulse action. Therefore, the present calculations mainly show the possibility of forming metastable regions during laser treatment. More precise study of such phenomena requires additional experimental research and the development of new mathematical models. At present, the practical conclusion is mainly that numerical simulation predicts the conditions for the appearance of metastable states. From a general point of view, it is necessary to compare the lifetime of the metastable phase (τ_{met}) and the duration of the sub-surface overheating (τ_{over}). If $\tau_{\mathrm{met}} < \tau_{\mathrm{over}}$, explosive decay of the metastable phase due to volumetric vapour formation is actually possible; as a result, the liquid droplets can break down the deposition process based on laser evaporation.

The dependence of heat process dynamics on laser wavelength (*i.e.* on the absorption coefficient χ) is the subject of complementary research. Just as an illustration of this strong influence, one can compare the

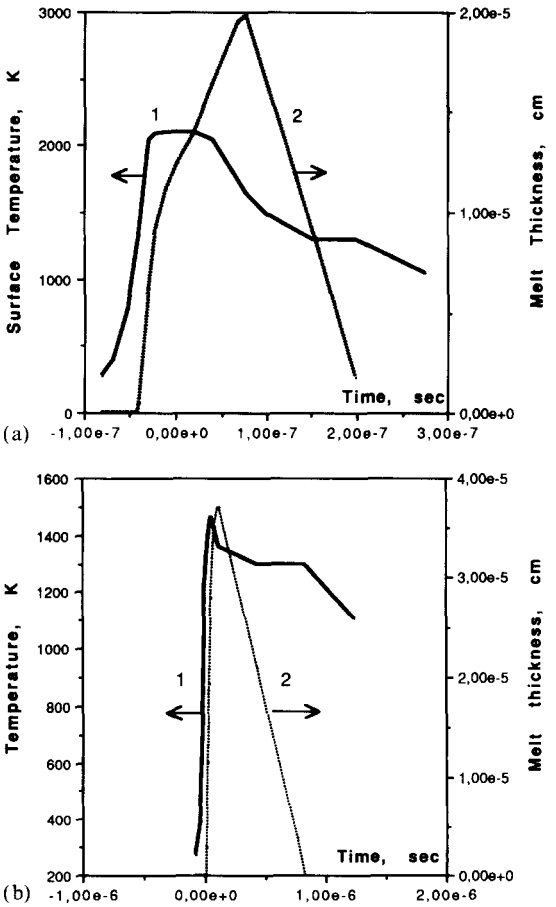

Fig. 3. Surface temperature (1) and melt thickness (2) *vs.* time: (a) surface absorption of laser radiation; (b) volumetric absorption coefficient $\chi = 10^4\ \mathrm{cm}^{-1}$. For both figures, $\tau = 40$ ns and $G_0 = 10^7\ \mathrm{W\,cm}^{-2}$.

maximum values of surface temperature, melt thickness and melt lifetime for (a) surface and (b) volumetric absorption for $\chi = 10^4\ \mathrm{cm}^{-1}$ (corresponding to a laser wavelength of about 1 μm), presented in Fig. 3. Note that the energy input is also a function of χ. The corresponding thickness of the evaporated layer per single pulse is 0.08 μm for surface absorption of radiation and 2×10^{-18} μm for $\chi = 10^4\ \mathrm{cm}^{-1}$. The considered range of variation of the absorption coefficient χ covers the range of laser wavelengths used in PLD.

5. Conclusions

1. The proposed mathematical model takes into account the kinetics of the melting and evaporation fronts under pulsed laser irradiation when volume absorption occurs. The evaporation process is described within the approximation of the Knudsen layer and melting on the basis of the Stefan type boundary condition.

2. The existence of a region in the solid phase where the temperature is higher than the melting point is shown. This is a consequence of the volumetric nature of energy release, on the one hand and of the melting phenomenon on the other when the interface temperature is fixed. The lifetime, the size of the metastable region and the degree of its overheating generally depend on the phase front dynamics and nucleation processes.

3. The occurrence of a sub-surface temperature maximum in the liquid phase is shown. This is the result of the volumetric nature of energy release on the one hand and of the evaporation phenomenon on the other hand when surface heat losses are intensive.

4. The formation of the overheated metastable states (in the range of parameters typical for pulsed laser deposition of superconducting films) can be the reason for splashing and therefore micron-sized particle generation.

5. The dependence of surface temperature, melt thickness, melt lifetime and thickness of evaporated layer on the absorption coefficient of laser radiation is illustrated in the range of wavelengths used in PLD.

References

1 D. B. Chrisey and A. Inam, *MRS Bull.*, *17* (1992) 37.
2 D. C. Paine and J. C. Bravman (eds.), Laser ablation for material synthesis, *Mater. Res. Symp. Proc.*, *191* (1990).
3 E. Fogarassy, C. Fuchs and S. de Unamuno, *Mater. Manuf. Processes*, *7* (1992) 31.
4 G. Carslaw and D. Jaeger, *Conduction of Heat in Solids*, 2nd edn., Oxford University Press, Oxford, 1959.
5 C. J. Knith, *AIAA J.*, *17* (1979) 519.
6 N. A. Dar'in and V. I. Mazhukin, *Differenzialnye uravnenija*, *23* (1987) 1154.
7 P. V. Breslavskij and V. I. Mazhukin, *Inzhenerno-fizicheskii jurnal*, *57* (1989) 107.
8 J. F. Thompson, *AJAA J.*, *22* (1984) 1505.
9 J. G. Verner, J. G. Blom and J. M. Sanz-Serna, *J. Comput. Phys.*, *82* (1989) 454.
10 M. Lacroix. *Num. Heat Transfer*, *B19* (1992) 57.
11 A. J. Wathen, *J. Comput. Phys.*, *101* (1992) 51.
12 V. I. Mazhukin, U. Semmler, P. V. Breslavskij and L. Yu. Takojeva, Das Programmpaket LASTEC-1 zur numerischen Simulation von Lasermaterialbearbeitungsprozessen, *Preprint* No 209/5. Jg. (1991).
13 A. Lashin, I. Smurov, A. Uglov, P. Matteazzi and V. Tagliaferri, *Int. J. Heat Technol.*, *7* (1989) 60.
14 I. Smurov, A. Uglov, A. Lashin, P. Matteazzi and V. Tagliaferri, *Int. J. Heat Mass Transfer*, *34* (1991) 961.
15 A. Uglov, I. Smurov, A. Lashin and A. Guskov, *Modelling of Thermal Processes under Pulsed Laser Action on Metals*, Nauka, Moscow, 1991.